# Effect of the mode of fixation of the thienyl rings on the electronic properties of electron acceptors based on indacenodithiophene (IDT)

Natalia Terenti, Andreea Petronela Crisan, Siriporn Jungsuttiwong, Niculina Daniela Hadade, Alexandra Pop, Ion Grosu, Jean Roncali

# Effect of the mode of fixation of the thienyl rings on the electronic properties of electron acceptors based on indacenodithiophene (IDT)

Natalia Terenti,[a] Andreea Petronela Crisan,[a] Siriporn Jungsuttiwong,[b] Niculina Daniela Hadade,[a] Alexandra Pop,[a] Ion Grosu,[a] Jean Roncali[a,c*]

- [a]Babes-Bolyai University, Faculty of Chemistry and Chemical Engineering, Department of Chemistry and SOOMCC, Cluj-Napoca, 11 Arany Janos str., 400028, Cluj-Napoca, Romania
- [b]Center for Organic Electronics and Alternative Energies, Department of Chemistry University of Ubon Ratchathani 34190, Thailand
- [c]Moltech Anjou CNRS, University of Angers, 2 Bd Lavoisier, 49045, Angers, France

* Corresponding author. E-mail address: jeanroncali@gmail.com (J. Roncali).

**Abstract**

Indacenodithiophene (IDT) is a major building block for the design of advanced functional π-conjugated polymers and nonfullerene electron-acceptor materials for organic photovoltaics. Preliminary results of a synthetic approach aiming at the modulation of the electronic properties of IDT-based acceptors by modification of the mode of linkage of the thiophene rings with the median phenyl ring are presented. The synthesis of three acceptor-donor-acceptor (A-D-A) structures corresponding to the different possible modes of thiophene-phenyl connection (**1-3)** Scheme 1) is described and their electronic properties are discussed on the basis of the results of UV-Vis absorption spectroscopy, cyclic voltammetry and theoretical calculations.

Keywords: indacenodithiophene; π-conjugated system; energy level; electron acceptor

## 1. Introduction

Organic photovoltaics (OPV) can potentially offer a low cost and low environmental impact complement, or even alternative, to solar cells based on inorganic semiconductors [1-4]. Several decades of multi-disciplinary research effort have produced a continuous increase of the conversion efficiency of OPV cells, leading to a progressive reduction of the gap between their performances and those of silicon solar cells [5]. During *ca* three decades, OPV cells have been fabricated with active materials which had not been specifically designed for PV conversion. Besides incremental research focused on the improvement of device fabrication, progress in OPV has been marked by several major qualitative steps such as the first planar donor-acceptor heterojunction (PHJ) in 1986 [2] or the invention of solution-processed bulk heterojunction (BHJ) ten years later [3,4]. On the other hand, the major advances accomplished during the past fifteen years are essentially due to the progress of the synthetic chemistry of active materials including low band gap polymers [6] molecular donors [7-9] and recently non-fullerene acceptors (NFAs) [10-14]. Since their introduction as active OPV material in the mid-nineties, fullerenes derivatives have represented the quasi-exclusive class of acceptor materials for both vacuum-deposited [15] and solution processed OPV cells [1,4]. However, fullerenes have some inherent limitations related to the cost of their synthesis and purification, their weak absorption in the visible region, and the difficult tuning of their energy levels. Although some NFAs were used before fullerenes in vacuum deposited PHJ cells [2,15-17], research on the design of soluble molecular acceptors for solution-processed BHJs is relatively recent [10-14]. Among the numerous molecular structures investigated, NFAs based on the indacenodithiophene (IDT) core have progressively emerged as very efficient materials [12-14,18] which have greatly contributed to the recent spectacular increase of the efficiency of BHJs now approaching 20 % [5]. However, in spite of this spectacular improvement of efficiency, the industrial development of OPV is still hampered by major problems related to the insufficient chemical and/or physical stability of the cells [19,20] and the cost and scalability of active materials [21,22]. The introduction of NFAs has generated major changes in the view of OPV cells. In “classical” fullerene-based BHJ cells, most of the light is absorbed by the donor material and charge generation proceeds essentially by photo-induced electron transfer from the donor to the acceptor (Channel I) [23]. The situation is different with NFAs since in many cases, a large part of light is absorbed by the acceptor while

charge generation can involve a significant contribution of photo-induced hole transfer from the acceptor to the donor (Channel II) [23].

Tetraaryl substituted indacenodithiophene IDT is a major building block for the design of advanced organic semiconductors [18]. Introduced in 2006 by Wong et al [24] IDT has been used for the synthesis of conjugated polymers [25-27] and more recently for the design of highly efficient NFAs [11-14,18,28,29]. In recent years many IDT-based NFAs have been synthesized and incorporated in highly efficient OPV cells and particularly in transparent OPV cells of high interest for building integrated photovoltaics (BIPV) [30-36]. The NFA-oriented chemistry of the IDT platform involves various approaches including the extension of the conjugated structure, the modification of electron-withdrawing end-blocks or of the aryl side-substituents [11-14,18,24, 28,29]. We report herein preliminary results related to a different strategy involving the modification of the mode of linkage of the thienyl heterocycles with the median phenyl ring on the electronic properties of the resulting electron-acceptor derivatives bearing dicyanovinyl (DCV) end groups. The synthesis of three molecules corresponding to three different modes of thiophene-phenyl connection is described (**1-3**, Scheme 1), and their electronic properties are discussed on the basis of the results of UV-Vis absorption spectroscopy, cyclic voltammetry and theoretical calculations.

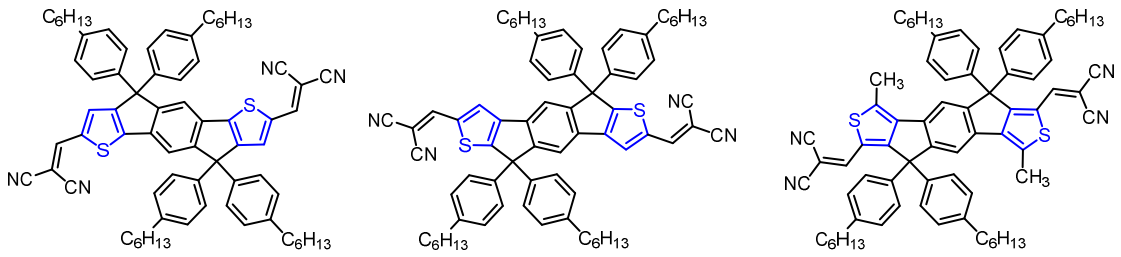


Scheme 1. Chemical structures of the target compounds **1-3**.

## 2. Results and discussion

*Synthesis*

The synthesis of compounds **1-3** is depicted in Scheme 2. Compound **1** was already described [37,38]. A Stille coupling of 2,5-dibromoterephthalate (**4**) with tributyl(thiophen-2-yl) stannane (**5**) gives diethyl 2,5-di(thiophen-2-yl) terephthalate (**6**) in 78 % yield. Treatment of 1-bromo-4-hexylbenzene (**7**) with butyllithium at -78°C gave the corresponding lithio-compound

which was then reacted with compound **6** to give after a double acid-promoted intramolecular cyclization reaction sequence, 4,4,9,9-tetrakis(4-hexylphenyl)-4,9-dihydro-s-indaceno[1,2-*b*:5,6-*b*']dithiophene (**8**) in 45 % yield. Vilsmeier formylation of compound **8** gave dicarbaldehyde (**9**) in 56% yield. A Suzuki coupling of **4** with thiophene-3-boronic acid pinacol ester (**11**) gave the corresponding dithienyl-terephalate (**12**) in 40% yield. Application of the lithiation/acid promoted cyclization sequence already used for **8** gave the indacenodithiophene **13** in 34% yield. This compound was then converted in 44 % yield into the corresponding dicarbaldehyde (**14**) by Vilsmeir formylation. A Suzuki coupling between 2,5-dibromoterephthalate (**4**) and the boronic ester **15** afforded compound **16** in 58% yield. The lithiation/acid promoted intramolecular cyclization sequence gave the indacenodithiophene **17** in 22 % yield. In this case, the 2-position of the thiophene ring was blocked by a methyl group in order to orient the subsequent cyclization towards the desired ring fusion through the less reactive 3 and 4 positions of the thienyl ring.

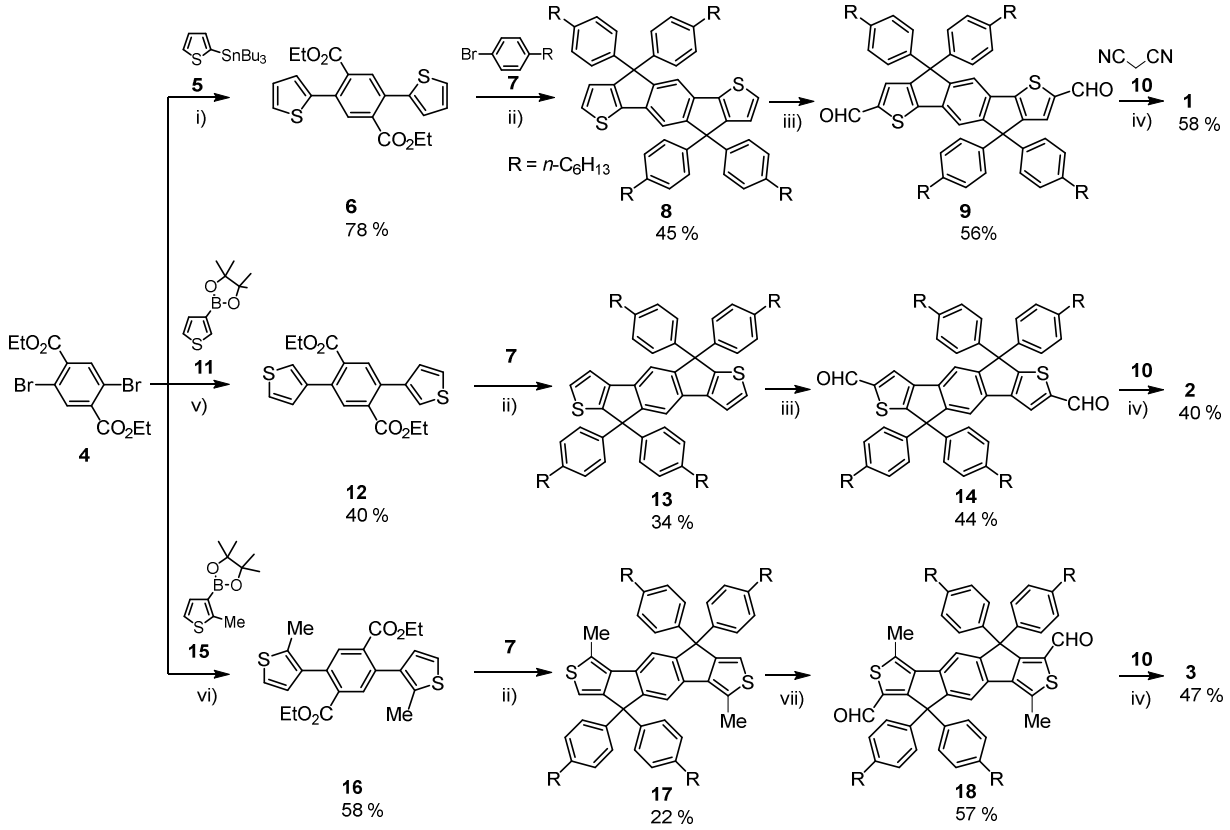


**Scheme 2**. Synthesis of the target compounds **1-3**. I) $Pd(PPh_3)_4$, toluene, 100°C, 24 h ; ii) *n*-BuLi, THF, -78°C, then $H_2SO_4$/AcOH rflx 4h iii) $POCl_3$, DMF, dichloroethane, 65°C, 12h; iv) malonodinitrile, pyridine, toluene rflx 3h; v) ) $Pd(PPh_3)_4$, $Cs_2CO_3$, toluene 100°C, 24 h; vi) ) $Pd(PPh_3)_4$, $Cs_2CO_3$, $Pd(dpp)Cl_2$, toluene 100°C, 48 h; vii) DCM, $TiCl_4$.

Compound **17** was then converted into dicarbaldehyde **18** by Rieche formylation using dichloromethyl ether in the presence of $TiCl_4$. The target compounds **1-3** were then obtained in 40-60% yield by Knovenagel condensation of dialdehydes **9**, **14** and **18** with malonodinitrile (**10**) in the presence of pyridine. The identity and purity of the three target molecules was confirmed by NMR and mass spectrometries.

*UV-Vis absorption spectroscopy*

Fig. 1 shows the UV-Vis absorption spectra of compounds **1-3** in DCM solution. The spectra of the three compounds exhibit a first transition in the 300-400 nm region and a second one in the 400-600 nm region for compound **1** and 400-500 for compound **2** and 400-450 nm for compound **3**.

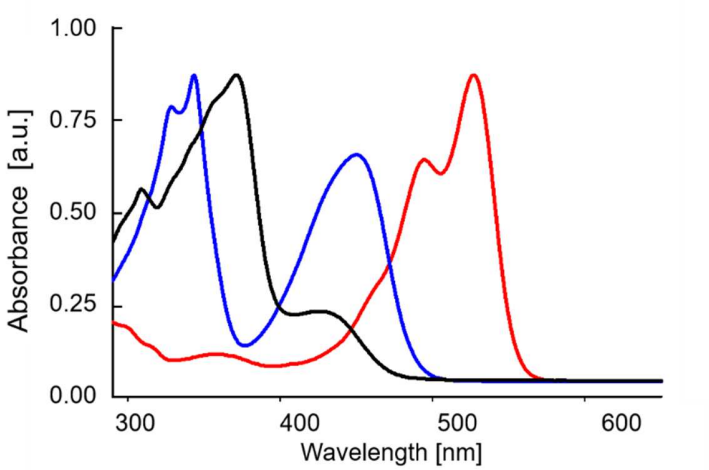


**Figure 1**. UV-Vis absorption spectra of compounds **1-3** in DCM solution. Red : **1**, blue: **2**, black: **3**.

Comparison with the spectra of compounds **8**, **13** and **17** (see SI) shows that the first transition can be assigned to the π–π* transition of the IDT unit whereas the absorption band at longer wavelengths corresponds to an internal charge transfer (ICT) between the electron-rich IDT core and the DCV electron-acceptor groups [39]. Comparison of the spectra of compounds **1-3** shows that the relative intensity of the ICT band *vs* that of the π–π* transition decreases dramatically from compound **1** to compound **3** leading to a complete inversion for compound **3**. Moreover, these modifications are accompanied by an hypsochromic shift of the ICT band with $\lambda_{max}$ shifting from 525 to 447 and 432 nm for **1**, **2** and **3** respectively (Table 1). On the other hand, the data in

Table 1 show that the optical gap $\Delta E_{opt}$ estimated from the absorption onset increase by 0.46 eV from 2.21 eV for **1** to 2.67 eV for **3**. These results show that the mode of linkage of the thienyl rings exerts a considerable influence on the optical gap of the system. Connection of the thienyl rings through a β-position limits the extent of electron delocalization over the whole acceptor-donor-acceptor (DAD) system by interrupting bond-length alternation due to the formation of two consecutive single bonds in the conjugated path of compounds **2** and **3** (Scheme 3). This restricted effective conjugation induces in turn a significant decrease of the strength of the ICT.

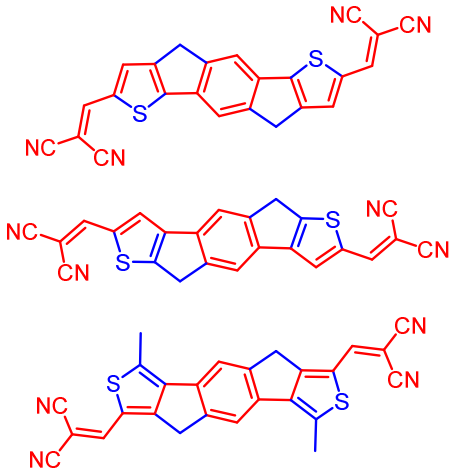


**Scheme 3.** Bond length alternation along the conjugated path in compounds **1**, **2** and **3** (from top to bottom).

The spectra of thin films of **1-3** spun-cast on glass are very similar to those of the DCM solutions with only small bathochromic shifts suggesting moderate intermolecular interactions in the solid state (see SI). The fluorescence emission spectra recorded in DCM solution show that the compounds are weakly emissive with emission maxima at 555, 535 and 495 nm (see SI) and quantum yields of 1.0, 0.80 and 0.30 % against rhodamine 6G for respectively **1**, **2** and **3**.

**Table 1**. Results of UV-Vis absorption spectroscopy[a] cyclic voltammetry[b] and estimated energy levels of the frontier orbitals for compounds **1-3**. [a:] in DCM solutions; [b:]in the conditions of Fig. 2.; [c:] from the long wavelength absorption edge; [d:] from the onset of oxidation and reduction waves using an offset of -4.68 eV for SCE [40].

| **Compd** | $\lambda_{max}$ (nm) | log $\varepsilon_{max}$ ($M^{-1}$ $cm^{-1}$) | $\lambda_{em}$ (nm) | $\Delta E_{opt}$[c] (eV) | $E_{pa}$ (V) | $E_{pc}$ (V) | $\Delta E_{elec}$ (eV) | $E_{HOMO}$[d] (eV) | $E_{LUMO}$[d] (eV) |
|---|---|---|---|---|---|---|---|---|---|
| **1** | 495, **525** | 4.52 | 555 | 2.21 | 1.39 | -0.94, -1.18 | 2.03 | -5.91 | -3.88 |
| **2** | 327, **342**, 447 | 4.71 | 535 | 2.51 | 1.47 | -0.99, -1.16 | 2.21 | -5.99 | -3.78 |

| | | | | | | | | | |
|---|---|---|---|---|---|---|---|---|---|
| **3** | 308, **372**, 432 | 4.86 | 495 | 2.67 | 1.52 | -1.05, -1.36 | 2.30 | -6.02 | -3.72 |

*Cyclic voltammetry*

The electrochemical properties of compounds **1-3** have been analyzed by cyclic voltammetry (CV) in DCM in the presence of $Bu_4NPF_6$ as the supporting electrolyte. The oxidation and reduction processes were investigated separately in order to prevent possible interferences between the process of interest (oxidation or reduction) and the eventual products of degradation of the opposite process

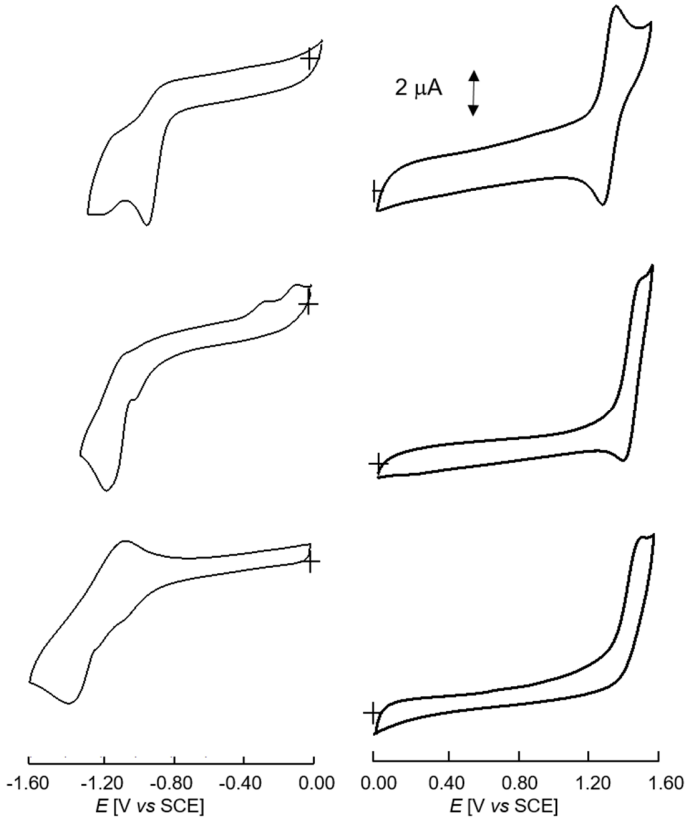


**Fig. 2.** Cyclic voltammograms of compounds **1-3** in 0.10 M $Bu_4NPF_6$/1:4 DCM/$CH_3CN$, Pt electrodes, scan rate 100 mV $s^{-1}$.

The CV of compound **1** shows a reversible one-electron oxidation wave with an anodic peak potential ($E_{pa}$) at 1.39 V corresponding to the formation of a stable radical cation. The clockwise rotation of the thiophene cycles relatively to the median phenyl ring produces a positive shift of $E_{pa}$ of 80 and 130 mV for **2** and **3** respectively with a loss of reversibility of the oxidation process. In the negative potential region, the CVs exhibit two successive reduction processes which are clearly apparent for compound **1** with cathodic peak potentials $E_{pc}1$ and $E_{pc}2$ at -0.94

and -1.18 V, while only weak shoulders preceeding the main reduction wave are observed for compounds **2** and **3**. Although these two processes probably correspond to the reduction of the DCV group and of the dithienyl-benzene system, further work such is needed to propose a clear assignment of the waves. The energy levels of the HOMO and LUMO were estimated using the onset of the oxidation and reduction processes. The electrochemical HOMO-LUMO gap ($\Delta E_{elec}$) derived from these estimated levels confirms, in agreement with optical data, an increase of the energy gap from **1** to **3** but the difference is only of 0.27 eV instead of 0.46 eV for $\Delta E_{opt}$. Furthermore, electrochemical data suggest that the increase of the gap involves a *quasi*-symmetrical decrease of HOMO level and increase of the LUMO level.

*Theoretical calculations*

In order to gain more information on these questions, quantum chemical calculations based on density functional methods have been performed on compounds **1-3** with the Gaussian 09 package. Becke's three-parameter gradient corrected functional (B3LYP) with 6-31G(d,p) basis was used to optimize the geometry and to compute the electronic structure. The optimized structures show that for all compounds the conjugated platform presents a fully planar geometry with, as expected, the phenyl-hexyl substituents in an almost orthogonal plane (Fig. 3). The calculated energy levels of the frontier orbitals clearly confirm that the modification of the mode of connection of the thienyl side groups exerts a strong influence on the energy gap with a predicted increase of $\Delta E$ of 0.63 eV between **1** and **3**, in satisfying agreement with the 0.46 eV value of $\Delta E_{opt}$. However, the computed results indicate that besides a small decrease of the HOMO level (0.12 eV) consistent with CV data, the increase of $\Delta E$ results essentially from a large increase of the LUMO level (0.50 eV). This discrepancy with CV results could be due to the fact that the reduction of the compounds involves two processes of quite different nature, namely the reduction of the DCV group and the formation of a radical anion on the rigid conjugated structure. Although only the latter process is relevant regarding charge separation and transport in the context of OPV conversion, a simple CV experiment does not allow to discriminate between these two processes. More generally, this poses the problem of the use of the onset of the first reduction (or oxidation) waves for the evaluation of HOMO and LUMO level of functional π-conjugated systems undergoing multiple redox processes of different nature.

To the best of our knowledge, this critical question is hardly considered in the abundant OPV literature.

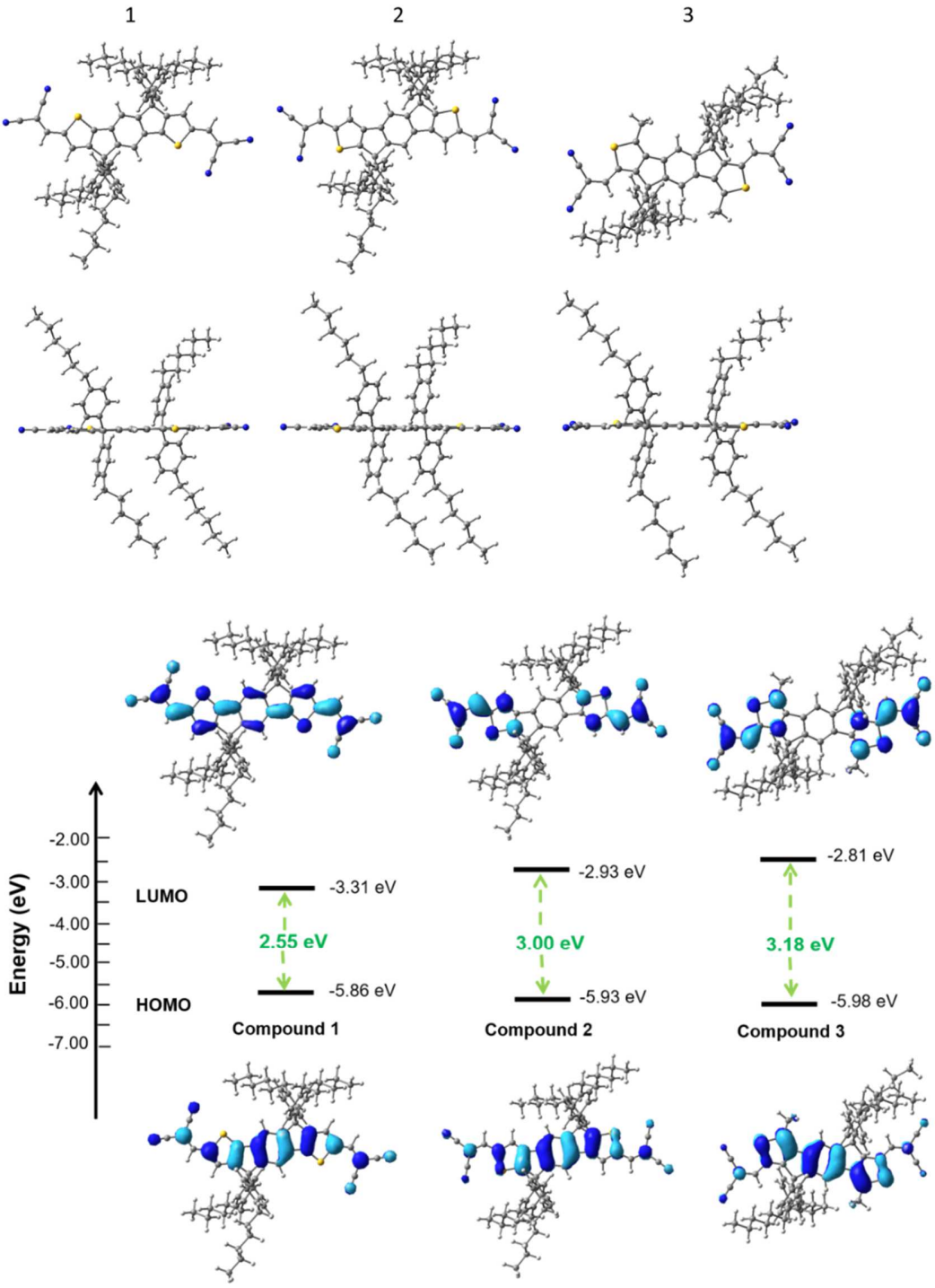


**Fig. 3.** Optimized geometries (top) and distribution of the HOMO and LUMO for compounds **1-3**.

*X-ray diffraction*

Single crystals of compound **2** (and **14** see SI) suitable for X-ray diffraction analysis have been obtained by slow evaporation of 2 :1 petroleum ether/ethylacetate solutions. However, attemps to obtain good quality crystals of compounds **1** and **3** have remained unsuccesfull. Fig. 4 shows the crystallographic structure of compound **2** [41]. The IDT-DCV conjugated system is perfectly planar with both DCV units in S-*cis* configuration. In the lattice each molecule interacts with two neighbors disposed on both sides of the IDT unit. These interactions involve in each case half of the molecule. The IDT units involved in the contacts are parallel (d=3.543Å) and the π-stacked IDT-DCV structures exhibit head-to tail orientations in parallel planes.

In addition a contact between the N atom of a cyano group and the ortho H atom of one of the *p*-hexyl-phenylene substituents (H---N = 2.6344 Å) is observed. The lattice shows layers of stacked fused aromatic units and associations among the layers are ensured by hydrophobic contacts of the hexyl groups.

## 3. Conclusion

Three A-D-A molecules involving dicyanovinyl electron-withdrawing groups attached on an indacenodithiophene electron-rich rigid platform have been synthesized in order to investigate the influence of the mode of linkage of the thienyl moieties on the central phenyl ring on the electronic properties of the resulting A-D-A systems. UV-Vis absorption spectroscopy reveals large changes of the optical properties and light transmission in the visible region with a *ca* 0.50 eV increase of the optical gap resulting from the modulation of the ICT. While cyclic voltammetry confirms the increase of the energy gap for compounds **2** and **3** with thiophenes connected to the phenyl group through a *β*-position, theoretical results clearly indicate that this effect is essentially due to an increase of the LUMO level. In spite of the large variations of their optical properties, the energy levels of these compounds remains in the same range of many highly efficient NFAs and are thus in principle compatible with a large number of donor materials for OPV [12-14, 23]. Of course, these criteria are not sufficient and the possible use of the new compounds as acceptors in OPV requires that the resulting solid-state materials fulfill

several other prerequisites in terms of exciton diffusion length, charge separation and charge transport. Work aiming at the scaling-up of the synthesis of these new structures in view of the analysis of these various aspects of their solid-state physics is now in progress and will be reported in future publications.

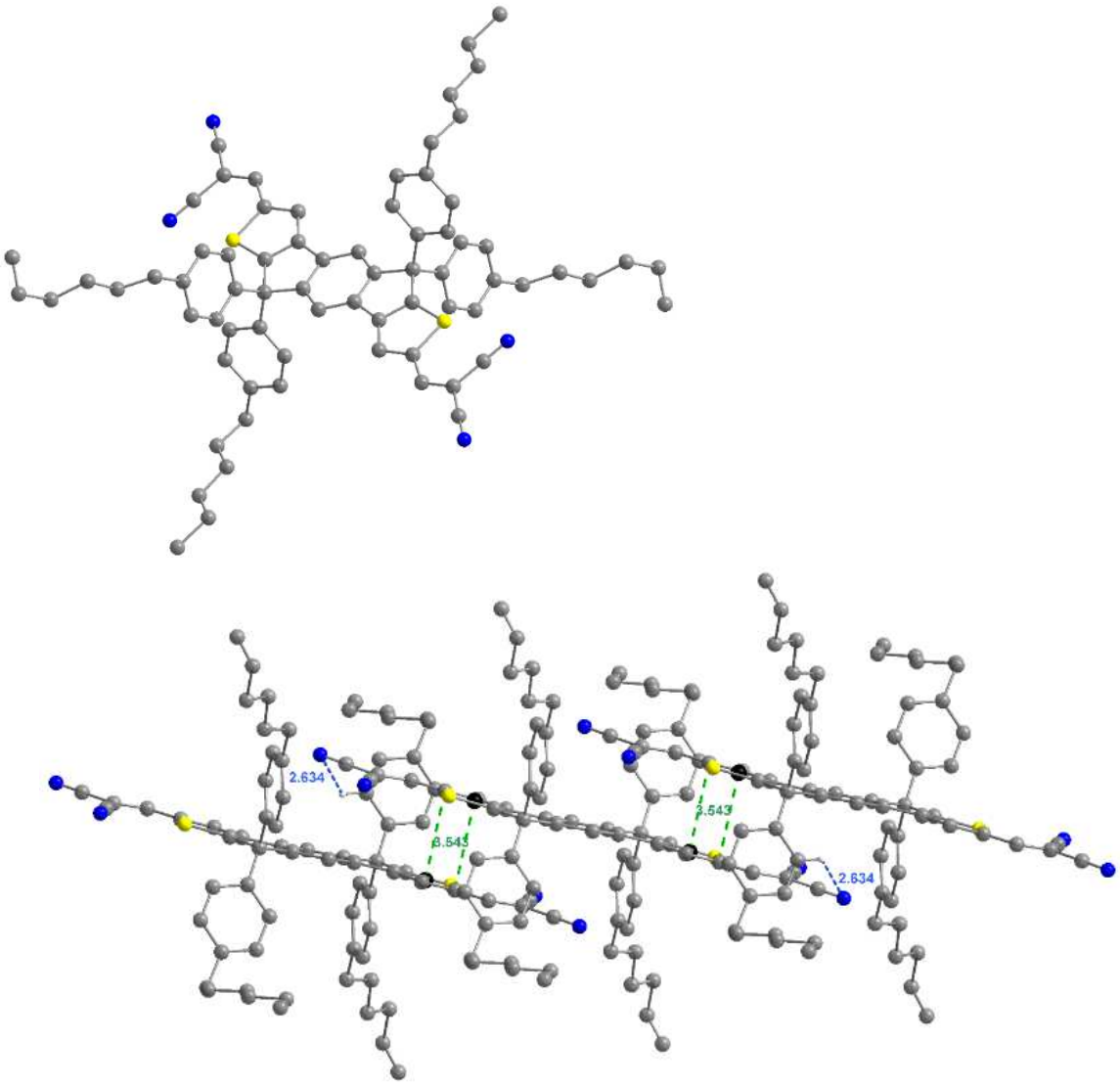


**Fig. 4**. Crystallographic structure of compound **2**.

*Experimental part*

***Diethyl-2,5-di(thiophen-2-yl)terephthalate*** (**6**). In a round-bottom flask containing 25 mL of dry toluene were added diethyl 2,5-dibromoterephthalate (**4**) (200 mg, 0.52 mmol) and tributyl(thiophen-2-yl) stannane (590 mg, 1.56 mmol). The mixture was degassed with argon and $Pd(PPh_3)_4$ (30 mg, 0.026 mmol) was added. The mixture was refluxed for 24 h and cooled to r.t. 20 mL of KF solution (0.1 g $mL^{-1}$) were added and the mixture was stirred at r.t. overnight. Water (60 mL) was added and the mixture was extracted with $CHCl_3$. The organic phase was dried over $MgSO_4$. After solvent removal, the residue was chromatographed on silica gel with 8:1 petroleum ether (PE)/AcOEt ($R_f$ = 0.36) as eluent yielding a white solid (158 mg, 79 %). M.p. 108-109 ºC. $^1$H NMR (400 MHz, $CDCl_3$), δ (ppm): 7.81 (s, 2 H), 7.39 (dd, *J* = 2.4 Hz, *J* = 7.2 Hz, 2 H), 7.08 (overlapped signals, 4 H), 4.21 (q, *J* = 10.8 Hz, 4H), 1.15 (t, *J* = 10.8 Hz, 6 H). $^{13}$C NMR (100 MHz, $CDCl_3$), δ (ppm): 167.9, 140.6, 134.2, 133.6, 132.0, 127.5, 127.1, 126.6, 61.8, 13.9. HRMS (APCI+): Calcd for $C_{20}H_{19}S_2O_4$ $[M+H]^+$:, 387.0719, found 387.0736.

***4,4,9,9-tetrakis(4-hexylphenyl)-4,9-dihydro-s-indaceno[1,2-b:5,6-b']dithiophene*** (**8**). *n*-butyllithium (2.70 mmol, 2.5 M) was slowly added to a stirred solution of 1-bromo-4-hexylbenzene (**7**) (655 mg, 2.70 mmol) in dry THF at -78ºC under argon atmosphere. After 1 h stirring at -78ºC a solution of **6** (150 mg, 0.39 mmol) in 2 mL of dry THF was added dropwise and the mixture was stirred 1h at -78°C and then allowed to cool to r.t. The reaction was quenched with water and the compound was extracted with AcOEt. The organic phase was washed with brine and dried over $MgSO_4$. After solvent removal the crude product was dissolved in 15 mL acetic acid and stirred 20 min at r.t. 0.05 mL of concentrated sulfuric acid was added, and the mixture was refluxed for 4 h. The mixture was cooled to r.t. and water was added. The mixture was extracted with DCM, the organic phase was washed with brine and dried over $MgSO_4$. After solvent removal the residue was chromatographed on silica gel (eluent: 8:0.5 PE/AcOEt, $R_f$ = 0.42). Compound **8** was isolated in 45 % yield as a white solid (158 mg). M.p. 157-158 ºC. $^1$H NMR (600 MHz, $CDCl_3$), δ (ppm): 7.43 (s, 2 H), 7.24 (d, *J* = 4.8 Hz, 2 H), 7.15 (d, *J* = 7.2 Hz, 8 H), 7.05 (d, *J* = 7.2 Hz, 8 H), 6.99 (d, *J* = 4.8 Hz, 2 H), 2.55 (t, *J* = 7.8 Hz, 8 H), 1.58 (m, 8 H), 1.34-1.28 (overlapped signals, 24 H), 0.87 (m, 12 H). $^{13}$C NMR (150 MHz, $CDCl_3$), δ (ppm): 155.9, 153.5, 142.2, 141.5, 141.4, 135.2, 128.4, 128.0, 127.5, 123.3, 117.6, 68.8, 35.7, 31.8, 31.5, 29.3, 22.7, 14.3. HRMS (ESI+): Calcd for $C_{64}H_{75}S_2$ $[M+H]^+$: 907.5305, found 907.5261.

***4,4,9,9-tetrakis(4-hexylphenyl)-4,9-dihydro-s-indaceno[1,2-b:5,6-b']dithiophene-2,7-dicarbaldehyde*** **(9).** To a solution of compound **8** (150 mg, 0.165 mmol) in 10 mL of 1,2-dichloroethane $POCl_3$ (126 mg, 0.825 mmol) and DMF (0.060 mg, 0.825 mmol) were added at 0°C. The mixture was kept at 0ºC for 1h and refluxed for 12 h under argon atmosphere. After cooled to r.t. a saturated sodium acetate solution (20 mL) was added and the mixture was stirred

for 30 min. The mixture was diluted with water and extracted with DCM. The organic phase was dried over $MgSO_4$. After solvent removal the crude product was chromatographed (4:3 DCM/PE $R_f$ = 0.28) to afford a yellow solid (84 mg, 56 %). M.p. 227-228 °C. $^1$H NMR (600 MHz, $CDCl_3$), δ (ppm): 9.82 (s, 2 H), 7.66 (s, 2 H), 7.59 (s, 2 H), 7.12 (d, *J* = 8.4 Hz, 8 H), 7.08 (d, *J* = 8.4 Hz, 8 H), 2.56 (t, *J* = 7.8 Hz, 8 H), 1.57 (m, 8 H), 1.34-1.27 (overlapped signals, 24 H), 0.87 (m, 12 H). $^{13}$C NMR (150 MHz, $CDCl_3$), δ (ppm): 183.0, 157.1, 155.3, 150.5, 146.6, 142.4, 140.7, 136.1, 132.2, 128.8, 127.8, 119.3, 63.1, 35.7, 31.9, 31.5, 29.3, 22.7, 14.2. HRMS (APCI+): Calcd for $C_{64}H_{75}S_2O_2$ $[M+H]^+$ 963.5203, found 963.5223.

***2,2'-((4,4,9,9-tetrakis(4-hexylphenyl)-4,9-dihydro-s-indaceno[1,2-b:5,6-b']dithiophene-2,7-diyl)bis(methanylylidene))dimalononitrile*** **(1)**. To a solution of **9** (50 mg, 0.051 mmol) and malononitrile (**10**) (13 mg, 0.20 mmol) in dry toluene (8 mL) three drops of pyridine were added. The mixture was refluxed for 3 h. After return to r.t. the mixture was quenched with water and extracted with DCM. The product was chromatographed, eluent:3:4 DCM/PE, ($R_f$ = 0.52) to give 32 mg (58%) ) of an orange solid. M.p. 308-309 °C. $^1$H NMR (600 MHz, $CDCl_3$), δ (ppm): 7.76 (s, 2 H), 7.61 (s, 2 H), 7.57 (s, 2 H), 7.08 (overlapped signals, 16 H), 2.56 (t, *J* = 7.8 Hz, 8 H), 1.58 (m, 8 H), 1.34-1.27 (overlapped signals, 24 H), 0.87 (m, 12 H). $^{13}$C NMR (150 MHz, $CDCl_3$), δ (ppm): 157.9, 156.0, 153.4, 151.1, 142.7, 140.0, 138.9, 136.2, 134.2, 128.9, 127.6, 119.8, 114.4, 113.8, 75.7, 63.2, 35.6, 31.8, 31.4, 29.2, 22.7, 14.2. HRMS (APCI+): Calcd for $C_{72}H_{75}N_4S_2$ $[M+H]^+$:, 1059.5428, found 1059.5477.

***Diethyl 2,5-di(thiophen-3-yl)terephthalate*** **(12)**. A mixture of **4** (400 mg, 1.04 mmol) and thiophene-3-boronic acid pinacol ester (**11**) (884 mg, 4.20 mmol) in dry toluene (20 mL) and aqueous 2 M $Cs_2CO_3$ (10 mL) was degassed with argon. $Pd(PPh_3)_4$ (60 mg, 0.052 mmol) was added and the mixture was stirred at 110 °C for 24 h under argon atmosphere. After cooling to r.t., and solvent removal the residue was solubilized in chloroform and washed with water and brine. The organic layer was dried over $MgSO_4$ and solvent removal. The crude product was chromatographed on silica gel with 8:1 PE/AcOEt ($R_f$ = 0.36) to give 162 mg, (40 %) of the target compound. M.p. 113-114 °C. $^1$H NMR (400 MHz, $CDCl_3$), δ (ppm): 7.80 (s, 2 H), 7.36 (m, 2 H), 7.31 (dd, *J* = 1.2 Hz, *J* = 2.8 Hz, 2 H), 7.12 (dd, *J* = 1.2 Hz, *J* = 4.8 Hz, 2 H), 4.12 (q, *J* = 3.2 Hz, 4 H), 1.32 (t, *J* = 3.2 Hz, 6 H). $^{13}$C NMR (100 MHz, $CDCl_3$), δ (ppm): 168.1, 140.3, 135.6, 133.7, 131.6, 128.6, 123.5, 123.0, 61.6, 14.0. HRMS (APCI+): Calcd for $C_{20}H_{19}S_2O_4$ $[M+H]^+$:, 387.0719, found 387.0726.

***5,5,10,10-tetrakis(4-hexylphenyl)-5,10-dihydro-s-indaceno[2,1-b:6,5-b']dithiophene*** **(13)**. *n*-Butyllithium (2.18 mmol, 2.5 M) was slowly added to a stirred solution of **7** (524 mg, 2.18 mmol) in dry THF (25 mL) at -78°C. After 1h, a solution of **12** (120 mg, 0.31 mmol) in 4 mL of dry THF was added dropwise. The mixture was stirred 1h at -78°C then allowed to return to r.t. and stirred overnight. The reaction was quenched with water and extracted with AcOEt. The organic phase was dried over $MgSO_4$. After solvent removal the product was dissolved in 40 mL acetic acid and stirred for 20 min. Three drops of concentrated sulfuric acid were added and the mixture was refluxed for 4 h. After cooling to r.t, water was added, the solution was extracted with DCM, the organic phase was washed with brine and dried over $MgSO_4$. After solvent removal the crude product was chromatographed on silica gel with 8:0.5 PE/AcOEt ($R_f$ = 0.42) to

afford 96 mg (38%) of white solid. M.p. 174-175°C. $^1$H NMR (600 MHz, $CDCl_3$), δ (ppm): 7.50 (s,2 H), 7.36 (d, *J* = 5.4 Hz, 2 H), 7.20 (d, *J* = 8.4 Hz, 8 H), 7.16 (d, *J* = 5.4 Hz, 2 H), 7.36 (d, *J* = 8.4 Hz, 8 H), 2.57 (t, *J* = 7.8 Hz, 8 H), 1.60 (m, 8 H), 1.36-1.29 (overlapped signals, 24 H), 0.89 (m, 12 H). $^{13}$C NMR (150 MHz, $CDCl_3$), δ (ppm): 154.1, 155.9, 144.9, 142.8, 141.6, 135.2, 129.9, 128.4, 128.0, 118.5, 118.2, 63.6, 35.7, 31.9, 31.5, 29.3, 22.7, 14.2. HRMS (APCI+): Calcd for $C_{64}H_{75}S_2$ $[M+H]^+$:, 907.5305 , found 907.5318.

***5,5,10,10-tetrakis(4-hexylphenyl)-5,10-dihydro-s-indaceno[2,1-b:6,5-b']dithiophene-2,7-dicarbaldehyde*** **(14).** $POCl_3$ (85 mg, 0.55 mmol) and DMF (40 mg, 0.55 mmol) were added at 0°C to a solution of **13** (100 mg, 0.11 mmol) in 1,2-dichloroethane (15 mL). After 1 h at 0°C, the reaction mixture was heated at 65°C for 12 h. After return to r.t., the reaction mixture was poured into ice water, neutralized with $Na_2CO_3$, and extracted with DCM. The organic phase was washed with brine and dried over $MgSO_4$. After removal of the solvent, the crude product was chromatographed on silica gel with 4:3 DCM/PE ($R_f$ = 0.28) to give 46 mg, (44 %) of a light yellow powder. M.p. 270-271°C. $^1$H NMR (600 MHz, $CDCl_3$), δ (ppm): 9.88 (s, 2 H), 7.82 (s, 2 H), 7.54 (s, 2 H), 7.13 (d, *J* = 7.8 Hz, 8 H), 7.07 (d, *J* = 7.8 Hz, 8 H), 2.56 (t, *J* = 7.8 Hz, 8 H), 1.58 (m, 8 H), 1.33-1.25 (overlapped signals, 24 H), 0.87 (t, *J* = 6.6 Hz, 12 H). $^{13}$C NMR (150 MHz, $CDCl_3$), δ (ppm): 183.2, 164.8, 153.7, 148.5, 145.4, 142.4, 141.5, 134.8, 128.8, 127.9, 127.4, 118.7, 64.5, 35.7, 31.8, 31.5, 29.2, 22.7, 14.2. HRMS (APCI+): Calcd for $C_{66}H_{75}S_2O_2$ $[M+H]^+$:, 963.5203, found. 963,5256.

***2,2'-((5,5,10,10-tetrakis(4-hexylphenyl)-5,10-dihydro-s-indaceno[2,1-b:6,5-b']dithiophene-2,7-diyl)bis(methanylylidene))dimalononitrile*** **(2)**. 0.1 mL pyridine was added under argon atmosphere to a solution of **14** (40 mg, 0.038 mmol) and **10** (10 mg, 0.015 mmol) in dry toluene (8 mL). The reaction mixture was refluxed for 3 h. After solvent removal, water (50 mL) and $CHCl_3$ (50 mL) were added. The aqueous layer was extracted with $CHCl_3$. The organic layer was washed with brine and dried over $MgSO_4$. The crude product was chromatographed on silica gel using 3:4 DCM/PE ($R_f$ = 0.52) to give 18 mg ( 40 %) of a light orange solid. M.p. 311-312°C. $^1$H NMR (600 MHz, $CDCl_3$), δ (ppm): 7.86 (s, 2 H) 7.72 (s, 2 H), 7.56 (s, 2 H), 7.11 (overlapped signals, 16 H), 2.57 (t, *J* = 7.8 Hz, 8 H), 1.68 (m, 8 H), 1.34-1.24 (overlapped signals, 24 H), 0.87 (m, 12 H). $^{13}$C NMR (150 MHz, $CDCl_3$), δ (ppm): 168.2, 154.0, 151.0, 146.3, 142.8, 140.7, 140.2, 134.4, 129.0, 127.9, 127.8, 119.2, 114.2, 113.5, 76.8, 65.1, 35.7, 31.8, 31.5, 29.2, 22.7, 14.2. HRMS (APCI+): Calcd for $C_{72}H_{75}N_4S_2$ $[M+H]^+$:, 1059.5428, found 1059.5480.

***Diethyl 2,5-bis(2-methylthiophen-3-yl)terephthalate*** **(16)**. A mixture of **4** (400 mg, 1.05 mmol), 4,4,5,5-tetramethyl-2-(2-methylthiophen-3-yl)-1,3,2-dioxaborolane (**15**) (944 mg, 4.2 mmol) in 20 mL dry toluene and aqueous 2 M $Cs_2CO_3$ (10 mL) was degassed with argon for 30 min. Pd(dppf)$Cl_2$ (38 mg, 0.053 mmol) was added and the mixture was heated at 110°C for 48 h under argon atmosphere. The reaction mixture was cooled to r.t, diluted with water and extracted with $Et_2O$. The ether phase was washed with brine and dried over $MgSO_4$. The crude product was chromatographed on silica gel with 10:1 pentane/AcOEt ($R_f$ = 0.63) to give 253 mg (58%) of a white solid. M.p. 119-120°C. $^1$H NMR (400 MHz, $CDCl_3$), δ (ppm): 7.78 (s, 2 H), 7.10 (d, *J* = 5.2 Hz, 2 H), 6.09 (d, *J* = 5.2 Hz, 2 H), 4.14 (q, *J* = 7.2 Hz, 4 H), 2.32 (s, 2 H), 1.10 (t, *J* = 7.2 Hz,

6 H). $^{13}$C NMR (150 MHz, $CDCl_3$), δ (ppm): 167.5, 136.9, 136.2, 135.2, 134.3, 132.7, 129.3, 121.4, 61.5, 13.9, 13.8. HRMS (APCI+) : Calcd for $C_{22}H_{23}S_2O_4$ $[M+H]^+$:, 415.1032, found 415.1004.

***5,5,10,10-tetrakis(4-hexylphenyl)-3,8-dimethyl-5,10-dihydro-s-indaceno[1,2-c:5,6-c']dithiophene*** **(17)**. To a solution of **7** (360 mg, 1.49 mmol) in dry THF (40 mL), cooled to -78 °C, was added dropwise under $N_2$ atmosphere 2.4 M *n*-butyllithium in hexane (1.49 mmol). The mixture was stirred for 1 h at -78 °C and a solution of **16** (200 mg, 0.21 mmol) in dry THF (6 mL) was added dropwise. After 1 h, the reaction was warmed to r.t., stirred overnight, poured into water and extracted with DCM. The organic phase was dried over $MgSO_4$. After removal of the solvent, acetic acid (50 mL) and concentrated $H_2SO_4$ (0.5 mL) were added and the mixture was refluxed for 4 h. Then, the mixture was poured into water and extracted with DCM. The resulting crude compound was chromatographed on silica gel with 4:0.5 pentane/DCM ($R_f$ = 0.4) as eluent to give 100 mg, (22%) of a white solid. M.p. 183-184ºC. $^1$H NMR (400 MHz, $CDCl_3$), δ (ppm): 7.52 (s, 2 H), 7.17 (d, *J* = 8.0 Hz, 8 H), 7.04 (d, *J* = 8.0 Hz, 8 H), 6.69 (s, 2 H), 2.55 (overlapped signals, 14 H), 1.57 (m, 8 H), 1.34-1.28 (overlapped signals, 24 H), 0.87 (m, 12 H). $^{13}$C NMR (100 MHz, $CDCl_3$), δ (ppm): 155.5, 154.4, 144.4, 141.1, 140.7, 135.2, 128.3, 128.1, 127.9, 119.9, 114.2, 60.9, 35.7, 31.9, 31.5, 29.3, 22.8, 14.3, 14.1. HRMS (APCI+): Calcd for $C_{66}H_{78}S_2$ $[M+H]^+$:, 935.5618, found 935.5663.

***5,5,10,10-tetrakis(4-hexylphenyl)-3,8-dimethyl-5,10-dihydro-s-indaceno[1,2-c:5,6-c']dithiophene-1,6-dicarbaldehyde*** **(18)**. A solution of **17** (80 mg, 0.085 mmol) in dry DCM (8 ml) was cooled to 0º C and $TiCl_4$ (42 mg, 0.222 mmol) was added dropwise under argon atmosphere The solution was stirred 1 h at 0ºC and dichloromethyl methyl ether (26 mg, 0.22 mmol) was added dropwise. The mixture was further stirred for 1 h at 0º C and then allowed to warm to r.t. After stirring overnight at r.t. the solution was poured into ice water and stirred for 30 min. After extraction with DCM, the organic phase was dried over $MgSO_4$, evaporated, and the crude product was chromatographed on silica gel with 1:2 $CHCl_3$/PE ($R_f$ = 0.6). Yield 48 mg, (57 %). M.p. 278-279ºC. $^1$H NMR (400 MHz, $CDCl_3$), δ (ppm): 9.75 (s, 2 H), 7.50 (s, 2 H), 7.18 (d, *J* = 8.0 Hz, 8 H), 7.08 (d, *J* = 8.0 Hz, 8 H), 2.65 (s, 6 H), 2.56 (t, *J* = 4.0 Hz, 8 H), 1.58 (m, 8 H), 1.35-1.25 (overlapped signals, 24 H), 0.87 (m, 12 H). $^{13}$C NMR (100 MHz, $CDCl_3$), δ (ppm): 182.6, 162.5, 156.3, 142.6, 142.2, 141.7, 139.4, 135.1, 131.3, 128.8, 128.3, 118.7, 62.7, 35.6, 31.8, 31.4, 29.2, 22.7, 15.2, 14.2. HRMS (APCI+): Calcd for $C_{68}H_{79}O_2S_2$ $[M+H]^+$: 991.5516, found 991.5584.

***2,2'-((5,5,10,10-tetrakis(4-hexylphenyl)-3,8-dimethyl-5,10-dihydro-s-indaceno[1,2-c:5,6-c']dithiophene-1,6-diyl)bis(methanylylidene))dimalononitrile*** **(3)**. Pyridine (0.1 mL) was added to a mixture of **18** (30 mg, 0.027 mmol) and **10** (7 mg, 0.110 mmol) in 6 mL dry toluene. The reaction mixture was refluxed for 6 h. After cooling to r.t, and solvent removal the crude product was chromatographed on silica gel with 3:4 DCM/PE (Rf = 0.57) to give 15 mg (47%) of the target compound. M.p. 315-316ºC; $^1$H NMR (400 MHz, $CDCl_3$), δ (ppm): 7.63 (s, 2 H), 7.48 (s, 2 H), 7.11 (overlapped signals, 16 H), 2.70 (s, 6 H), 2.59 (t, *J* = 8.0 Hz, 8 H), 1.62 (m, 8 H), 1.37-1.30 (overlapped signals, 24 H), 0.88 (t, *J* = 6.4 Hz, 12 H). $^{13}$C NMR (100 MHz, $CDCl_3$), δ

(ppm): 165.3, 157.1, 149.0, 142.8, 142.4, 141.1, 140.1, 134.8, 129.1, 128.1, 124.5, 118.7, 114.5, 113.5, 75.9, 62.9, 35.7, 31.8, 31.3, 29.3, 22.7, 15.3, 14.2. HRMS (APCI+): Calcd for $C_{72}H_{75}N_4S_2$ $[M+H]^+$:, 1087.5741, found 1087.5781.

**Declaration of competing interest**

No conflict of interest.

**Acknowledgments**

This work was financially supported by the project SMOSCs, ID: 37_220, Cod MySMIS:103509 funded by the Romanian Ministry for European Funds through the National Authority for Scientific Research and Innovation (ANCSI) and co-funded by the European Regional Development Fund/Competitiveness Operational Program 2014-2020 (POC) Priority Axis 1/Action 1.1.4.

[1] Günes S, Neugebauer H, Sariciftci NS, Conjugated polymers based organic solar cells, Chem Rev 2007; 107: 1324.

[2] Tang C W. Two-layer organic photovoltaic cell. Appl Phys Lett 1986; 48: 183.

[3] Halls J J M, Walsh C A, Greenham N C, Marseglia E A, Friend R H, Moratti S C, Holmes A B. Efficient photodiodes from interpenetrating polymer networks. Nature 1995; 376: 498.

[4] Yu G, Gao J, Hummelen J C, Wudl F, Heeger A J. Polymer Photovoltaic Cells: Enhanced Efficiencies via a Network of Internal Donor-Acceptor Heterojunctions. Science 1995; 270: 1789.

[5] Zhang J, Xian K, Zhang T, Hong L, Wang Y, Xu Y, Ma K, An C, He C, Wie Z, Gao F, Hou J. Cui Y, Yao H. Single-Junction Organic Photovoltaic Cells with Approaching 18% Efficiency. Adv Mater 2020; 32: 1908205.

[6] Cheng Y-J, Yang S-H, Hsu C-S, Synthesis of Conjugated Polymers for Organic Solar Cell Applications, Chem Rev 2009; 109: 5868.

[7] Roncali J. Molecular bulk heterojunctions: an emerging approach to organic solar cells. Acc Chem Res 2009; 42: 1719.

[8] Mishra A, Baüerle P. Small molecules organic semiconductors on the move: promises for future solar energy technology, Angew Chem Int Ed. 2012; 51: 2020.

[9] Collins SD, Ran NA, Heiber TC, Nguyen T-Q, Small is Powerful: Recent Progress in Solution-Processed Small Molecule Solar Cells. Adv Energy Mater 2017; 7: 1602242.

[10] Eftaiha A F, Sun J-P, Hill I G, Welch G C. Recent advances of non-fullerene, small molecular acceptors for solution processed bulk heterojunction solar cell. J Mater Chem A 2014; 2: 1201.

[11] Lin Y, Zhan X. Non-fullerene acceptors for organic photovoltaics: an emerging horizon, Mater Horiz 2014; 1: 470.

[12] Cheng P, Li G, Zhan X, Yang. Next-generation organic photovoltaics based on non-fullerene acceptors. Nature Photonics 2018; 12: 131.

[13] Zhang G, Zhao J, Chow P C Y, Jiang K, Zhang J, Zhu Z, Zhang J, Huang F, Yan H. Non fullerene acceptors molecules for bulk heterojunction organic solar cells. Chem Rev 2018; 118: 3447.

[14] Hou J, Inganäs O, Friend R, Gao F, Organic solar cells based on non-fullerene acceptors, Nature Mater 2018; 17: 119.

[15] Peumans P, Yakimov A, Forrest S. Small molecular weight organic thin-film photodetectors and solar cells. J Appl Phys 2003; 93: 3693.

[16] Wörle D, Meissner D. Organic solar cells, Adv Mater 1991; 3: 129.

[17] De Bettignies R, Nicolas Y, Blanchard P, Levillain E, Nunzi J-M, Roncali J, Planarized Star-shaped Oligothiophenes as Organic Semi-Conductors for Efficient Heterojunction Solar Cells. Adv Mater 2003; 15: 1939.

[18] Li Y, Gu M, Pan Z, Zhang B, Yang X, Gu J, Chen Y, Indacenodithiophene: A Promising Building Block for High Performance Polymer Solar Cells, J Mater Chem A 2017; 5:10798.

[19] Cheng P, Zhan X W, Stability of organic solar cells: challenges and strategies, Chem Soc Rev 2016; 45: 2544.

[20] Roncali J, Grosu I. The dawn of single-material organic solar cells. Adv Sci 2019; 6: 1801026.

[21] Po R, Bianchi G, Carbonera C, Pellegrino. “All That Glisters Is Not Gold”: An Analysis of the Synthetic Complexity of Efficient Polymer Donors for Polymer Solar Cells. Macromolecules 2015; 48: 453.

[22] Po R, Roncali J. Beyond efficiency: scalability of molecular donors for organic photovoltaics. J Mater Chem C 2016; 4: 477.

[23] Stoltzfus D M, Donaghey J E, Armin A, Shaw P E, Burn P L, Meredith P, Charge Generation Pathways in Organic Solar Cells: Assessing the Contribution from the Electron Acceptor. Chem Rev 2016; 116: 12920.

[24] Wong K-T, Chao T-C, Chi L-C, Chu Y-Y, Balaiah A, Chiu S-F, Liu Y-H, Wang Y, Syntheses and Structures of Novel Heteroarene-Fused Coplanar π-Conjugated Chromophores, Org Lett 2006; 8: 5033.

[25] Chen C-P, Chan S-H, Chao T-C, Ting C, Ko B-T. Low-Bandgap Poly(Thiophene-Phenylene-Thiophene) Derivatives with Broaden Absorption Spectra for Use in High-Performance Bulk-Heterojunction Polymer Solar Cells. J. Am Chem Soc 2008 ;130 :12828.

[26] Chan S-H, Chen C-P, Chao T-C, Ting C, Lin C-S, Ko B-T. Synthesis, Characterization, and Photovoltaic Properties of Novel Semiconducting Polymers with Thiophene-Phenylene-Thiophene (TPT) as Coplanar Units. Macromolecules 2008 ; 41: 5519.

[27] Zhang W, Smith J, Scott E. Watkins S E, Gysel R, McGehee M, Salleo A, Kirkpatrick J, Ashraf S, Anthopoulos T, Heeney M, McCulloch I. Indacenodithiophene Semiconducting Polymers for High Performance, Air-Stable Transistors J Am Chem Soc 2010; 132: 11437.

[28] Lin Y, Wang J, Zhang Z G, Bai H, Li Y, Zhu D, Zhan X, An electron acceptor challenging fullerene for efficient polymer solar cells. Adv Mater 2015; 27: 1170.

[29] Wu Y, Bai H, Wang Z, Cheng P, Zhu S, Wang Y, Ma W, Zhan X, A planar electron acceptor for efficient polymer solar cells, Energy Environ Sci 2015; 8: 3215.

[30] Traverse C J, Pandey R, Barr M C, Lunt R R, Emergence of highly transparent photovoltaics for distributed applications, Nature Energy 2017; 2: 849.

[31] Lee K, Um H-D, Choi D, Park J, Kim N, Kim H, Seo K, The development of transparent photovoltaics. Cell Reports 2020; 1: 100143.

[32] Chang S-Y, Cheng P, Li G, Yang Y. Transparent polymer photovoltaics for solar energy harvesting and beyond. Joule 2018; 2: 1039.

[33] Sun C, Xia R, Shi H, Yao H, Liu X, Hou J, Huang F, Yip H-L, Cao Y, Heat-Insulating Multifunctional Semitransparent Polymer Solar Cells. Joule 2018; 2: 1.

[34] Wang D, Qin R, Zhou G, Li X, Xia R, Li Y, Zhan L. High-Performance Semitransparent Organic Solar Cells with Excellent Infrared Reflection and See-Through Functions. Adv Mater 2020: 2001621.

[35] Cui Y, Yang C, Yao H, Zhu J, Wang Y, Jia G, Gao F, Hou J. Efficient Semitransparent Organic Solar Cells with Tunable Color enabled by an Ultralow Bandgap Nonfullerene Acceptor. Adv Mater 2017; 1703080.

[36] Cheng P, Yang Y, Narrowing the Band Gap: The Key to High-Performance Organic Photovoltaics. Acc Chem Res 2020; 53:1218.

[37] Ko EY, Park GE, Lee JH, Kim HJ, Lee DH, Ahn H, Uddin MA, Woo HY, Cho MJ, Choi DH. Excellent Long-Term Stability of Power Conversion Efficiency in Non-Fullerene-Based Polymer Solar Cells Bearing Tricyanovinylene-Functionalized n-Type Small Molecules. ACS Appl Mater Interfaces, 2017; 9: 8838.

[38] Yin X, Zhong F, Chen Z, Gao C, Xie G, Wang L, Yang C. Manipulating the Doping Level via Host-dopant Synergism towards High Performance n-type Thermoelectric Composites. Chem Eng J 2020; 382: 122817.

[39] Roquet S, Cravino A, Leriche P, Alévêque O, Frère P, Roncali J. Triphenylamine-thienylenevinylenes Hybrid Systems with Internal Charge-transfer as Donor Material for Hetero-junction Solar Cells J Am Chem Soc 2006; 128: 3459.

[40] Trasatti S, The Absolute Electrode Potential: An Explanatory Note, Pure Appl Chem 1986; 58: 955.

[41] CCDC-2038967 (**2**) and CCDC-2038968 (**12**) contain the supplementary crystallographic data for this paper. These data can be obtained free of charge from The Cambridge Crystallographic Data Centre via www.ccdc.cam.ac.uk/ data_request/cif.